Transcriptome Dysregulation in Hepatoblastoma: The Pivotal Role of Noncoding Rnas and Changes in Lipid Metabolism

Maria Prates Rivas
University of Sao Paulo: Universidade de Sao Paulo
Talita Ferreira Marques Aguiar (marquesaguiar@gmail.com)
Columbia University Medical Center: Columbia University Irving Medical Center https://orcid.org/0000-0003-0202-6848
Edson Mario de Andrade
Federal University of Vicosa: Universidade Federal de Vicosa
Sara Ferreira Pires
University of Sao Paulo: Universidade de Sao Paulo
Alexandre Defelicibus
Hospital AC Camargo: ACCamargo Cancer Center
Bruna Barros
Hospital AC Camargo: ACCamargo Cancer Center
Estela Novak
Sao Paulo University Faculty of Medicine: Universidade de Sao Paulo Faculdade de Medicina
Lilian Maria Cristofani
Sao Paulo University Faculty of Medicine: Universidade de Sao Paulo Faculdade de Medicina
Vicente Odone
Sao Paulo University Faculty of Medicine: Universidade de Sao Paulo Faculdade de Medicina
Monica Cypriano
Federal University of Sao Paulo: Universidade Federal de Sao Paulo
Silvia Regina Caminada de Toledo
Federal University of Sao Paulo: Universidade Federal de Sao Paulo
Isabela Werneck da Cunha
Rede D'Or: Rede D'Or Sao Luiz
Cecilia Maria Lima da Costa
Hospital AC Camargo: ACCamargo Cancer Center
Dirce Maria Carraro
Hospital AC Camargo: ACCamargo Cancer Center
Israel Tojal
Hospital AC Camargo: ACCamargo Cancer Center

Tiago Antônio de Oliveira Mendes
Federal University of Vicosa: Universidade Federal de Vicosa
Ana Cristina Victorino Krepischi
University of Sao Paulo: Universidade de Sao Paulo https://orcid.org/0000-0003-2931-8605

Research Article

Keywords: Hepatoblastoma, RNA-Seq, transcriptome, noncoding RNA, lipid, metabolism

Posted Date: April 19th, 2022

DOI: https://doi.org/10.21203/rs.3.rs-1538524/v1

Abstract

Hepatoblastoma, the most common liver tumor in children and exhibited the lowest mutational burden among solid cancers, pointing to chromosomal and epigenetic changes as the main drivers of tumorigenesis. Previous studies explored hepatoblastoma transcriptomes focusing on risk stratification, but no consensual molecular signature emerged. We performed whole-transcriptome analysis with total RNA sequencing using 14 hepatoblastomas compared with control liver samples. A set of 1,492 differentially expressed genes (DEGs) was detected, 1,031 upregulated and 461 downregulated, comprising 920 protein-coding genes (62%). A strong dysregulation of non-coding RNA genes (ncRNAs) was revealed, mostly upregulated. Among the top 50 genes with the highest expression, 42% of them were ncRNAs, and three (*MAGED4, SNO144-16*, and *RP11-431J24.2*) were exclusively expressed by hepatoblastomas. Upregulated biological processes were linked to cell differentiation, communication and signaling pathways, as well as embryonic and developmental processes. Enriched biological processes in downregulated genes included mainly negative regulation of oxidation and metabolism inhibition, affecting amine, nicotinamide, and lipids. An integrative analysis between miRNA-mRNA and protein-protein interaction networks highlighted major biological processes associated with metabolism and oxidation reactions of lipids and carbohydrates, methylation-dependent chromatin silencing, and DNA methylation. Four upregulated miRNAs (*miR-186*, *miR-214*, *miR-377*, and *miR-494*) were disclosed, potentially targeting more than 10 protein-coding transcripts, which suggested a possible role in their negative regulation. In conclusion, the RNASeq analysis revealed the disruption of metabolic pathways, including lipids, amines, and nicotinamides, and disclosed a robust ncRNA transcriptome perturbation, highlighting a new epigenetic player in the control of hepatoblastoma gene expression, along with DNA methylation.

Key Messages

- Whole-transcriptome analysis with total RNA sequencing using 14 hepatoblastomas compared with control liver samples.
- 1,492 differentially expressed genes (DEGs) was detected.
- 1,031 upregulated and 461 downregulated, comprising 920 protein-coding genes (62%).
- Among the top 50 genes with the highest expression, 42% of them were ncRNAs.
- RNASeq analysis revealed the disruption of metabolic pathways and disclosed a robust ncRNA transcriptome perturbation.

Introduction

Cancer is a complex condition driven by the acquisition of an increasing number of genomic changes at diverse levels of complexity [1]. Hepatoblastoma (HBL), the most common childhood liver cancer, stand out as the solid tumor with the lowest rate of somatic mutations, presenting 1–7 single nucleotide variant (SNV) per tumor genome [2, 3]. This finding clearly points to a tumorigenesis that mostly reliant on larger

chromosomal gains and losses [4–8] and epigenetic changes [9–11].Currently, there is no widely used HBL classification, given the clinical and genetic heterogeneity, and the already suggested prognostic biomarkers presented reproducibility limitations [10, 12–15]. Thus, the search for key biological pathways involved in HBL development and progression yet is a challenge to the field.

Ultimately, all driver genomic changes in cancer, such as point mutations and chromosomal aberrations as well as epigenetic modifications, will result in crucial deviations of genome expression in a particular cell/tissue type, and their impact can best be captured by evaluating the pattern of downstream molecules, including RNA, protein, and metabolites [16, 17]. RNA sequencing (RNA-seq) is a widespread next-generation sequencing technique, which provides an unbiased global picture of the gene expression, being successfully applied to reveal the molecular bases of many oncological diseases [18, 19]. Only a few groups have explored the HBL transcriptome using RNA-seq, the first of them proposing a HBL stratification model based on the expression pattern of four genes (*HSD17B6, ITGA6, TOP2A*, and *VIM*) [14]. Recently, HBL transcriptome data were integrated with methylome and genomic analyses, disclosing hypomethylation and overexpression of the 14q32 *DLK1/DIO3* locus as a possible marker of aggressiveness [10]. Sekiguchi et al. also integrated multiomics analyses leading to the clusterization of HBLs in groups according to the stage of tumor cell differentiation [12].

Beyond changes in protein-coding genes mainly associated with the WNT pathway and hepatocyte differentiation markers, the role of non-coding RNAs (ncRNA) is poorly explored in HBL transcriptomes. About 85% of the human genome is transcribed in some extent as ncRNA [20, 21], which is a gene category composed of two major classes, the small non-coding RNAs (sncRNAs) and long non-coding RNAs (lncRNAs) [22]. In HBLs, there are isolated and remarkable examples of the potential relevance of ncRNAs. *MEG3/MEG8* (2 maternally expressed non-coding genes), and small nucleolar RNAs of the C/D box family (namely *SNORD113* and S*NORD114*) were suggested for classification of tumor aggressiveness [10], and isolated sncRNAs have been associated with tumor suppression or oncogenic activity in HBL, with prognostic value [23].

Metabolic dysfunction driven by genomic changes is also largely unknown in HBLs. Recently, we demonstrated in HBLs the downregulation of *NNMT* [24], an enzyme responsible for the nicotinamide N-methylation process which is linked with metabolic pathways in hepatocytes [25]. An untargeted metabolomics analysis detected a reduction in the lipid content of HBLs, possibly associated with the NNMT downregulation and suggesting a connection with a worse prognosis [24].

In the present HBL transcriptome study, the analysis revealed a central role for the downregulation of metabolic pathways, mostly associated with lipid reduction, and a global ncRNA upregulation.

Materials And Methods

Tumor specimens and RNA extraction

Fourteen fresh-frozen primary HBLs and five control liver samples (non-tumoral matched liver tissues) were surgically obtained between 2016–2019 from patients enrolled in three Brazilian cancer institutions: A.C. Camargo Cancer Center, GRAACC, and ITACI (São Paulo, SP, Brazil). Clinical data are summarized in **Table 1**. This study was approved by the Research Ethics Committee of the respective institutions, and samples were collected after signed informed consent from patients' parents or legal guardians. Total RNA samples were isolated using the RNeasy Mini Kit (Qiagen, Hilden, Germany), according to the manufacturer's protocol. Microfluidics-based electrophoresis (Bioanalyzer, Agilent Technologies, USA) was performed to verify the RNA quality, and only samples with RIN (RNA Integrity Number) ≥ 7.0 were used.

RNA sequencing and alignment

The total RNA extracted from the 19 liver samples was used to build cDNA libraries using the TruSeq®Stranded Total RNA LT- kit (with Ribo-Zero TM Gold) (Illumina, USA). Sequencing was performed on the NextSeq 500 platform Mid Output v2 Kit (150 cycles) (Illumina, USA).The FASTQ files were aligned against the ribosomal reference sequence (NCBI, 12/2017) using the BWA software [26]version 0.7.17-r1188, in MEM mode, with the standard parameters, except for the -t 4 parameters. Reads not aligned to ribosomal sequences went to the alignment step against the reference sequence of the human genome (version GRCh37 - hg19) using the STAR software [27], version 2.6.1a_08–27. All samples presented a minimum of 5 million reads, and the reading count per gene was calculated using the HTSeq software [28]version 0.11.2. The annotation database (GTF file) used was the Ensembl file in version 87 in the same build as the human genome reference (GRCh37). The FPKM metrics were used to normalize the count with a Python 3 script developed by the Bioinformatics Laboratory of the A. C. Camargo Cancer Center. All the analyses were performed by comparing HBLs *versus* control liver samples.

Principal Component Analysis (PCA)

A PCA analysis was performed using the FPKM values, on a $\log_{10}$ scale, with the function *prcomp* [29]. The ideal number of clusters was determined by the function *fviz_nbclust*, and the PCA representation, with the definition of the clusters, was generated with the function *fviz_cluster* of the *factoextra* package [30]. In addition, the summary of contributions for the first 10 components was obtained using the function f*viz_contrib*, from the *factoextra* package.

Differential Gene Expression Analysis

Differential gene expression analysis was performed using DEseq2 software [31] version 1.18.1, available in the Bioconductor package for R version 3.4.1, following the good practices listed in the Standard Workflow available in the literature [32]. The parameters used in this analysis were: *test_method Wald*, *fit_method parametric*, *padj BH*, and *normalization vst*. For the calculation of saturation and expression, minimum coverage of 1 (one) read was considered. Cutoff values of 0.05 for the adjusted p-value (FDR) and $\log_2$ fold-change < -1 or > 1 were applied for selection of a robust list of differentially expressed genes (DEGs).

The result of the differential expression analysis was summarized in a volcano plot. The $\log_2$ values of fold-change and FDR generated by DESeq2 were used for plotting the graph in an R environment with the functions plot, point, and textxy [29, 33]. A Venn diagram was elaborate to depict the number of shared or exclusive transcripts from the DEGs in tumor and control liver samples. A heatmap was used to analyze the expression profile and group the DEGs. The gene expression levels were normalized by FPKM and converted to a z-score scale before using the *Heatmap* function, from the *ComplexHeatmap* package, in an R environment [34], with the parameter km = 3. The Manhattan plot was used to represent the genomic mapping of DEGs to autosomal chromosomes and their respective $\log_2$ fold-change and FDR values. In this analysis, we only considered the FDR value (< 0.05) as a cutoff to define the up or down regulated genes. This analysis was implemented with command line routines in bash/awk and an R environment, with tools from the *karyoploteR* package [35]. We also assessed cytobands with over-represented up or down-regulated genes in relation to the genome; cytoband coordinates were obtained from the H. sapiens (human) genome assembly GRCh37 (hg19), with the plotKaryotype function from the karyoploteR package [35]. These coordinates were used, together with the GFF file (also for the GRCh37 genome), to identify the genes mapped to each cytoband, and the total up/down regulated genes by cytobands of each chromosome were counted to obtain a contingency table, using Python scripts. The contingency table obtained was used in Fisher's exact test, with the *fisher.test* function (at the 5% significance level), followed by adjust P-values for multiple comparisons with Bonferroni method using the *p.adjust* function, in R environment. This was made comparing the number of up or down regulated genes in each cytoband with the total number of up or down regulated genes in the genome, respectively.

Gene annotation enrichment analysis

An analysis of functional enrichment was performed with the set of the up and downregulated DEGs. This analysis was carried out with the *enrichGO* function of the *clusterProfiler* package, with the parameters: *de, OrgDb = "org.Hs.eg.db", ont = "all"* [36]. Furthermore, the *dot plot* function was used to plot the main enriched biological processes, cellular components, and molecular functions considering this set of genes. To identify the tendency of a given biological process to be increased (mainly up-regulated genes) or reduced (mainly down-regulated genes), an analysis with the *GOplot* package (using the *GOCircle* and *GOChord* functions) was performed. In addition, a functional enrichment analysis was performed using Cytoscape's BiNGO plugin, with the list of DEGs as input (the BiNGO default settings were maintained). The output of BiNGO was formatted, using Python script and bash/awk routine, according to the standard required by GOplot [37]. Thus, the circular diagram (GOCircle) was obtained to represent ten relevant biological processes. Also, a string diagram (GOChord) was obtained to represent the genes in the processes shown in the GOCircle which have the biggest fold-changes. This information was used to generate a summarized network in which were represented only the interactions of proteins encoded by the DEGs, their centralities, clusters, and enriched biological processes.

miRNA-mRNA interaction network

Based on the miRNAs and mRNAs with differential expression, a miRNA-mRNA interaction network was built. Data from the miRTarBase [38]and TargetScan databases were used [39]. Interactions between

differentially expressed miRNA and lncRNA were identified using data from the miRcode database [40]. The miRNA-mRNA interactions of these databases were joined with the Merge Network tool of the Cytoscape program, and the interactions between differentially expressed miRNAs and mRNAs were selected using routine commands in bash/awk. The main enriched biological processes were represented in a dot plot, obtained with the *dot plot* function of the *clusterProfiler* package.

Protein-protein-miRNA Interaction (PPI)

A study based on protein-protein interaction networks was conducted to determine centrality and identify the relevant functional modules with proteins encoded by DEGs. The network of *H. sapiens* was downloaded from the STRING database and the interactions were filtered (confidence greater than 900) for subsequent analyses. The central proteins for the system (Hub, Bottleneck, and Hub-Bottleneck) were identified using analysis for the *betweenness* centrality and degree, with the functions *betweenness* and *degree* of the igraph package [38]. Those proteins were categorized into i) common (C): the *degree and betweenness* values were below the global average of the network; ii) hub (H): the degree value was above the global average of the network; iii) bottleneck (B): the value for *betweenness* centrality was above the global average value of the network; and iv) hub-bottleneck: both the degree and betweenness values were higher than the global network average. A subnet for first-degree interactions of proteins encoded by DEGs was used in the cluster analysis in an R environment, applying the *fastgreedy.community* function [41]. The identification and selection of biological enriched functional processes of protein clusters were performed using the BiNGO plugin from the Cytoscape program [42], followed by protein selection associated with relevant biological processes. Interactions between miRNA with mRNA encoding central proteins in interatomic were represented as miRNA-protein interaction, to highlight the existence of miRNA-mRNA.

Results

The clinical features of the cohort of the 14 patients with HBL are described in **Table 1.** The mean age at diagnosis was 24 months, excluding three atypical patients: one was diagnosed at 17 years (HB28), one at 12 years (HB38), and one at 7 years (HB39). Four patients were born premature (< 37 weeks), with low birth weight (< 900g). According to CHIC classification [43, 44], eight patients were diagnosed with high-risk HBL; four presented with pulmonary metastasis at diagnosis. All received neoadjuvant chemotherapy protocols followed by tumor resection or transplantation. Four patients died due to the primary disease and one patient (HB39) died after a second primary tumor (fossa pilocytic astrocytoma).

PCA and cluster analyses showed that two groups were the optimal number to clustering the liver samples (**Supplementary Material S1**). The differential expression analysis detected 1492 DEGs (FDR < 0.05 and $\log_2$ fold-change < -1 or > 1) in HBLs compared to control liver samples (**Supplementary Table S1)**. The heatmap analysis based on the DEGs supported the existence of two major sample clusters, one of them exclusively composed of HBLs, and a second one containing all control liver samples plus one HBL (Fig. 1A). The Fig. 1B corresponds to the PCA based on the DEGs highlighting the two major

identified clusters and the respective grouped samples. To show the genomic mapping of the DEGs, we used the Manhattan plot (Fig. 1C), which exhibited an even distribution of the DEGs along all autosomal chromosomes; however, one cluster of upregulated genes could be highlighted at the cytoband 14q32.31 (q-value: 1.97e-16). For downregulated genes, there were no cytobands with significant enriched genes (data not shown).

Among the detected 1492 DEGs (**Table 2**), 1031 were upregulated and 461 were downregulated (Fig. 2A). The list of DEGs comprised 920 protein-coding genes (558 upregulated and 362 downregulated), corresponding to 62% of the total with changes in expression. Different classes of non-coding RNAs (ncRNAs) accounts for 22% of the total list of DGEs, mostly upregulated, such as 258 long ncRNAs (lcnRNAs) (199 upregulated and 59 downregulated), and 73 small ncRNAs (68 upregulated sncRNAs, of which 20 were miRNAs, and 5 downregulated); the remaining 16% of DEGs were classified as pseudogenes, and immunoglobulin genes. The Venn diagram presents the number of transcripts from the DEGs that presented shared or exclusive expression in the HBL and control liver groups (Fig. 2B). We found that 85 of the DEGs were exclusively expressed in HBL samples (**Supplementary Table S2)**, approximately 55% of them corresponding to ncRNAs.

Table 3 exhibits the top 50 genes defined as those with the highest expression changes in HBLs compared to control livers, 25 upregulated and 25 downregulated genes, with their associated information; 42% of them correspond to ncRNAs. Three genes among the top 50 list (*MAGED4*, *SNO144-16*, and *RP11-431J24.2*) were exclusively expressed in HBLs, none of them previously reported.

Figure 3A presents the major enriched up and down-regulated biological processes, cellular components, and molecular functions according to the list of genes with altered expression in HBLs. Ten selected biological processes which were found to be statistically disrupted in the HBL transcriptome are depicted in Fig. 3B in the GoCircle plot; it is possible to observe that biological processes presenting predominance of negative regulation were associated with reduced oxidation and metabolism inhibition, such as amine, nicotinamide, and lipid metabolism. Conversely, upregulated biological processes in HBLs were linked with the regulation of cell communication and signaling pathways, as well as cell differentiation, and embryonic and developmental processes. In the GoChord graph (Fig. 3C), nine of the enriched biological processes highlighted above are depicted with ten of the 50 top genes which are associated with them, five presenting increased expression in tumors and five with reduction. Only coding protein genes could be associated with biological processes.

The PPI network displayed 6431 nodes and 239279 connectors with *degree mean and betweenness* mean of 42.0 and 7026.0, respectively. In this network, seven clusters stood out, concerning the enriched biological processes (**Supplementary Material S2; Supplementary Table S3)**. From this network and analysis, it was possible to generate the subnet shown in Fig. 4, highlighting the interaction of central proteins coded by DEGs, among others. Centrality *betweenness and degree* measures showed that this subnet was composed of one hub protein (F13A1), nineteen bottleneck nodes (*ACADS, TH, HSD17B10, ECHS1, GSTZ1, SHMT1, GLS2, RBP2, MTR, NAT8L, ELOVL4, GGPS1, HES1, LIMD1, GCK, DCP2, MSH2,*

CAMK2B, and CNOT6) and eleven hub-bottleneck (*CDA, CCND1, HDAC2, CCNB1, AGO1, AKT1, IRF7, PSMB8, CD36, GNAL*, and *GPLD1*). The hub-bottleneck proteins are associated with clusters involved with biological processes of negative regulation of metabolism, DNA methylation, cytotoxicity, and signaling pathways, including cytokine-mediated signaling pathway.

Considering the large portion of deregulated ncRNAs, we built a miRNA-mRNA interaction network to explore a possible regulation of protein-coding genes in HBLs by miRNAs. In this analysis, the network predicts protein-coding mRNA with miRNAs based on miRTarBase and TargetScan databases. Using 18 out of 20 upregulated miRNAs in HBLs was possible to obtain a network with involvement of 30 processed upregulated miRNAs and 82 down regulated mRNAs (Fig. 5A). Among the miRNAs, four of them (miR-186, miR-214, miR-377, and miR-494; also present in Fig. 4) related to more than 10 mRNAs, suggesting an important role in the regulation of expression of these protein-coding genes. The analysis between lncRNA and miRNA, also presented in this Figure, evidenced that the upregulated miRNA-214 in HBL interacts with lncRNA differently expressed in tumors. The top 20 biological processes with the highest level of significance associated with the upregulated or downregulated mRNAs networks can be found in Fig. 5B and 5C, respectively; the major biological processes related to this miRNA-mRNA network are linked to down regulated mRNAs and associated with metabolism (10 processes) and oxidation reactions of lipids and carbohydrates (5 processes).

Discussion

We identified in HBL transcriptomes a central dysregulation of noncoding RNAs, associated with changes in the expression of genes linked to metabolism and oxidative reactions of lipids and carbohydrates. The assessment of these findings together with our previous data[24] reinforced that the disturbance of metabolic pathways in a major event in HBLs, besides disclosing an aberrant ncRNA network, which can be highlighted as a new epigenetic player in the control of gene expression of this tumor type, along with the already reported abnormal DNA methylation [9, 11, 45]

The analysis of the PCA and the heatmap showed two clusters of samples, one exclusively tumoral and the other composed of control liver samples but one tumor (79T). It is noteworthy that this particular tumor did not carry somatic coding mutations or copy number alterations, maybe explaining its similarity of expression with control livers. Four clusters with similar expression patterns were observed in HBLs, three of them consisting of upregulated genes affecting biological pathways associated with development, and morphogenesis, which is linked to the disruption of the differentiation proposed for HBL genesis [46–48]. Most of these increased processes are linked to developmental events, and associated with gene changes such as *DKK1* [49], *BMP4* [50], *RUNX2* [51], *LEF1* [52], as well as homeobox genes such as *DLX1, DLX6, MSX1* [53], among others. *HMGA2* and *CDH3* upregulation are associated with embryonic development, cell differentiation, and communication. *HMGA2* polymorphisms were recently linked to HBL progression [54]; and *CDH3* encodes a classical cadherin component of glycoproteins, and alterations were not described in HBL before. The overexpression of *DKK1* was reported in HBL as a novel biomarker related to uncontrolled wingless/WNT signaling [55]. We also

detected upregulation of *DKK4*, previously reported with increased expression in HBLs [56] and other cancers, such as colorectal, gastric, pancreatic, and renal; however, in hepatocellular carcinoma was observed a reduced *DKK4* expression, suggesting that effects of *DKK4* in tumorigenesis and progression can vary in the different tumors [57, 58].

On the other hand, the identified cluster 4, composed of downregulated genes, was linked to metabolic processes, revealing a crucial role of metabolism interference in HBLs. Changes in HBL metabolism are still poorly described and understood [59, 60]. *THRSP*, for example, a gene associated with lipid metabolism, was found to be downregulated in our data; it is expressed in liver and adipocytes, and we previously showed *THRSP* promoter hypermethylation in HBLs [11], suggesting that expression control by an epigenetic mechanism can interfere in the tumoral lipid metabolism. In addition, the observed downregulation of *TTC36* can be associated with alterations in the metabolism of amine and small molecules, development process, and cell differentiation. This gene is associated with tumor suppressor activities, and its inactivation in gastric cancer might promote cell proliferation, at least in part through activating the Wnt/β-catenin signaling pathway [61]. Another interesting gene for future studies is *GCK*, which contributes to the reprogramming of energy metabolism in cancer cells [57]. Recently, bioinformatic analyses of microarray expression in HBLs also highlighted changes in biological processes associated with small-molecule catabolism, organic acid metabolism, lipid metabolism, and oxidation-reduction reactions [62].

Differentially expressed genes in HBLs were found to be widely distributed on chromosomes, with only the 14q32 region showing an enriched cluster of upregulated genes. The overexpression of a 300 kb region located at the 14q32 DLK1/DIO3 locus, previously reported in association with DNA hypomethylation, indicates a direct role of this epigenetic mechanism in gene expression control [10]. In a previous study, this locus was associated with a major increase in the expression of a cluster of miRNAs and snoRNA of the C/D box family (namely *SNORD113* and *SNORD114*), especially in metastatic tumors [63]. Our data corroborated these recent findings regarding 14q32 locus overexpression on HBLs; we detected upregulation of the genes at this locus (*DLK1, MEG3, SNORD113-3, SNORD114-22*) that Carillo et. al proposed to classify HBLs according to the level of 14q32 gene expression.

Analysis of the protein network revealed which proteins encoded by DEGs were decisive in the pathways and mechanisms highlighted throughout this work. Increased *HDAC2* expression was detected, and this protein presents a hub-bottleneck centrality associated with methylation-dependent chromatin silence, DNA methylation, and negative regulation of metabolism. It is interesting to note that recent work showed epigenetic silencing by histone deacetylases (HDAC) as a critical step for the development of pediatric liver cancer [58]. Particularly, the elevation of HDAC1 and HDAC2 proteins were found in a large group of patients with HBLs [64]. Also classified as a hub-bottleneck centrality protein, *CCND1* presented downregulation in tumor samples; as a major regulator of the cell cycle transition, this protein reduction can directly interfere in cell proliferation. *CCND1* germline polymorphisms have been proposed as contributors of HBLs development [54]. CCND1 protein was associated in the network with methylation-dependent chromatin silence, DNA methylation, negative regulation of metabolism, leukocyte mediated

cytotoxicity, and cytokine-mediated signaling pathway. It is important to note that our data suggested a *CCND1* regulation by mir-494 in the miRNA-mRNA analysis. *GCK* and *CAMK2B*, downregulated in HBLs, were also classified with a centrality degree; the first one was associated with metabolism and cytokine pathways, and the second with epigenetic processes (DNA methylation and gene silencing) as well as cytokine-mediated signaling. The mRNAs *GCK* and *CAMK2B* were two of the ten genes emphasized in the GOcircle, and *CAMK2B* was predicted to be regulated by miR-186 in the miRNA-mRNA analysis. Therefore, *CCND1, GCK* and *CAMK2B* are strong candidates for future analyses.

From the 1,492 DEGs detected in HBLs, 85 were exclusively expressed in tumors, 47 of them being lncRNAs or miRNAs. Altered ncRNA expression has been observed in several tumor types, including colorectal [65], hepatocellular carcinoma [66], gastric [67], and renal cell carcinoma [68], indicating that aberrant expression of ncRNAs contributes to carcinogenesis. In HBLs, a previous study has shown that the microRNA profile can distinguish tumors from control liver tissues [69]. In our work, miRNAs found to be upregulated were associated with possible oncogenic activities through the putative regulation of downregulated mRNAs. Based on the miRNA-mRNA analysis, we propose that 18 of the differentially expressed miRNA precursors here detected in HBLs were linked with regulation of mRNA expression of 82 genes. It is important to clarify that this analysis is limited because not related to mature/processed miRNAs, and functional validation was not performed. Yet, the upregulation of four miRNA precursors (miR-186, miR-214, miR-377, and miR-494) detected in HBLs were central and could possibly result in reduced expression of their target protein-coding genes. In our HBL transcriptome data, the overexpression of miR-186 was predicted to be linked to 26 down-regulated mRNAs; recently, Cui et al. described miR-186 reduced expression targeting an N6-methyladenosine gene (*MTTL3*) and affecting HBL progression[61]. The upregulate miR-214 precursor was associated with the possible downregulation of 12 mRNAs; however, the literature reported opposite miR-214 downregulation[62, 70] a discrepancy that should be validated by other technique. The overexpression of miR-377 was predicted to be related to 22 down-regulated mRNA in HBLs, and recent publications supported this upregulation pattern [62, 71]. Lastly, the miR-494 precursor was potentially linked to the downregulation of 11 mRNA genes. The miRNA-494 is overexpressed in HCC (hepatocellular carcinoma), being considered an epigenetic regulator associated with tumor invasiveness, proliferation, and migration [72, 73], and linked to *TET1* activity and tumor progression [72]. We previously indicated an increased expression of the TET family genes (*TET1*, *TET2*, and *TET3*) in HBLs, connected with an active demethylation activity and increased 5hmC. Therefore, upregulation of miR-494 is a novelty in the HBL biology, and future studies can provide further links among its expression and *TET1* regulation.

Conclusion

The present work revealed key biological pathways in the transcriptome of HBL, evidencing a pivotal role of noncoding RNA dysregulation and reinforcing the disturbance of metabolic pathways as a major event in HBLs, according to our previous findings. Several relevant genes were proposed for future functional studies, including four upregulated miRNA precursors (miR-186, miR-214, miR-377, and miR-494) which were linked to reduced expression of at least ten protein-coding genes. Thus, the present work highlighted

a major disruption of metabolic homeostasis as well as a new epigenetic mechanism associated with ncRNA, particularly miRNAs, as future targets for understanding tumorigenesis in HBL.

Declarations

DATA AVAILABILITY STATEMENT

The original contributions presented in the study are included in the article/Supplementary Material, further inquiries can be directed to the corresponding author/s. Raw data was submitted to the GEO with the number of access: GSE199888 (https://www.ncbi.nlm.nih.gov/geo/query/acc.cgi?acc=GSE199888).

CONFLICTS OF INTEREST

The Authors declares that there is no conflict of interest.

FUNDING

The present study was supported by grants from FAPESP (CEPID - Human Genome and Stem Cell Research Center 2013/08028-1; 2018/21047-9; fellowships 2016/04785-0, 2016/23462-8). CAPES (88887.508357/2020-00) and CNPq (141625/2016-3). The funders had no roles in the study design, data collection and analysis, decision to publish, or preparation of the manuscript.

ETHICAL APPROVAL

Samples were recovered from patients enrolled in three Brazilian cancer institutions: A.C. Camargo Cancer Center, GRAACC and ITACI (São Paulo) The Research Ethics Committee of the respective Institutions approved this research using these biological samples, and all samples were collected after informed signed consent was obtained from parents or legal guardians.

CONTRIBUTORSHIP

MPR, TFMA, EMA, TAOM and ACVK conceived the study, and participated in its design; MPR, TFMA, SFP, AD, BB, IT, TAOM and ACVK performed the collection and assembly of data; MPR, TFMA, SFP, AD, BB, EN, LMC, VO, MC, SRCT, DMC, CMLC, IWC, IT, TAOM and ACVK realized the data analysis and interpretation; MPR, TFMA, EMA and ACVK wrote the manuscript; all authors have read and approved the final version of the manuscript.

ACKNOWLEDGEMENTS

We thank the patients and their families for participating in the study.

References

1. Vogelstein B, Papadopoulos N, Velculescu VE et al (2013) Cancer genome landscapes. Science 339:1546–1558. https://doi.org/10.1126/science.1235122
2. Gröbner SN, Worst BC, Weischenfeldt J et al (2018) The landscape of genomic alterations across childhood cancers. Nature 555:321–327. https://doi.org/10.1038/nature25480
3. Aguiar TFM, Rivas MP, Costa S et al (2020) Insights Into the Somatic Mutation Burden of Hepatoblastomas From Brazilian Patients. Front Oncol 10:556. https://doi.org/10.3389/fonc.2020.00556
4. Rodrigues TC, Fidalgo F, da Costa CML et al (2014) Upregulated genes at 2q24 gains as candidate oncogenes in hepatoblastomas. Future Oncol 10:2449–2457. https://doi.org/10.2217/fon.14.149
5. Harel T, Lupski JR (2018) Genomic disorders 20 years on—mechanisms for clinical manifestations. Clin. Genet
6. Villela D, Barros JS, da Costa SS et al (2020) Detection of mosaicism for segmental and whole chromosome imbalances by targeted sequencing. Ann Hum Genet ahg 12402. https://doi.org/10.1111/ahg.12402
7. Tomlinson GE, Douglass EC, Pollock BH et al (2005) Cytogenetic evaluation of a large series of hepatoblastomas: numerical abnormalities with recurring aberrations involving 1q12-q21. Genes Chromosomes Cancer 44:177–184. https://doi.org/10.1002/gcc.20227
8. Arai Y, Honda S, Haruta M et al (2010) Genome-wide analysis of allelic imbalances reveals 4q deletions as a poor prognostic factor and MDM4 amplification at 1q32.1 in hepatoblastoma. Genes Chromosomes Cancer 49:596–609. https://doi.org/10.1002/gcc.20770
9. Rivas MP, Aguiar TFM, Fernandes GR et al (2019) TET upregulation leads to 5-hydroxymethylation enrichment in hepatoblastoma. Front Genet 10. https://doi.org/10.3389/fgene.2019.00553
10. Carrillo-Reixach J, Torrens L, Simon-Coma M et al (2020) Epigenetic footprint enables molecular risk stratification of hepatoblastoma with clinical implications. J Hepatol 0. https://doi.org/10.1016/j.jhep.2020.03.025
11. Maschietto M, Rodrigues TC, Kashiwabara AY et al (2016) DNA methylation landscape of hepatoblastomas reveals arrest at early stages of liver differentiation and cancer-related alterations. https://doi.org/10.18632/oncotarget.14208. Oncotarget
12. Sekiguchi M, Seki M, Kawai T et al (2020) Integrated multiomics analysis of hepatoblastoma unravels its heterogeneity and provides novel druggable targets. https://doi.org/10.1038/s41698-020-0125-y. npj Precis Oncol
13. Cairo S, Armengol C, De Reynies A et al (2008) Hepatic stem-like phenotype and interplay of Wnt/beta-catenin and Myc signaling in aggressive childhood liver cancer. Cancer Cell 14:471–484. https://doi.org/10.1016/j.ccr.2008.11.002
14. Hooks KB, Audoux J, Fazli H et al (2018) New insights into diagnosis and therapeutic options for proliferative hepatoblastoma. Hepatology 68:89–102. https://doi.org/10.1002/hep.29672
15. Sumazin P, Chen Y, Treviño LR et al (2017) Genomic analysis of hepatoblastoma identifies distinct molecular and prognostic subgroups. Hepatology 65:104–121. https://doi.org/10.1002/hep.28888

16. Zhang S, Wei JS, Khan J (2013) The Significance of Transcriptome Sequencing in Personalized Cancer Medicine. From Bench to Personalized Medicine, In: Cancer Genomics
17. Gomez-Casati DF, Grisolía M, Busi MV (2016) The Significance of Metabolomics in Human Health. In: Medical and Health Genomics
18. Cieślik M, Chinnaiyan AM (2018) Cancer transcriptome profiling at the juncture of clinical translation.Nat. Rev. Genet
19. Hong M, Tao S, Zhang L et al (2020) RNA sequencing: new technologies and applications in cancer research. J. Hematol. Oncol
20. Jin D, Song Y, Chen Y, Zhang P (2020) Identification of Three lncRNAs as Potential Predictive Biomarkers of Lung Adenocarcinoma. Biomed Res Int. https://doi.org/10.1155/2020/7573689
21. Xie W, Yuan S, Sun Z, Li Y (2016) Long noncoding and circular RNAs in lung cancer: Advances and perspectives. Epigenomics
22. Ferreira HJ, Esteller M (2018) Non-coding RNAs, epigenetics, and cancer: tying it all together. Cancer Metastasis Rev. https://doi.org/10.1007/s10555-017-9715-8
23. Cristobal I, Sanz-Alvarez M, Luque M et al (2019) The Role of MicroRNAs in Hepatoblastoma Tumors. Cancers (Basel) 11:. https://doi.org/10.3390/cancers11030409
24. Rivas MP, Aguiar TFM, Maschietto M et al (2020) Hepatoblastomas exhibit marked NNMT downregulation driven by promoter DNA hypermethylation. Tumor Biol. https://doi.org/10.1177/1010428320977124
25. Kim J, Hong SJ, Lim EK et al (2009) Expression of nicotinamide N-methyltransferase in hepatocellular carcinoma is associated with poor prognosis. J Exp Clin Cancer Res. https://doi.org/10.1186/1756-9966-28-20
26. Li H (2013) [Heng Li - Compares BWA to other long read aligners like CUSHAW2] Aligning sequence reads, clone sequences and assembly contigs with BWA-MEM. arXiv Prepr arXiv
27. Dobin A, Davis CA, Schlesinger F et al (2013) STAR: Ultrafast universal RNA-seq aligner. Bioinformatics. https://doi.org/10.1093/bioinformatics/bts635
28. Anders S, Pyl PT, Huber W (2015) HTSeq-A Python framework to work with high-throughput sequencing data. Bioinformatics. https://doi.org/10.1093/bioinformatics/btu638
29. R: a language and environment for statistical computing
30. Alboukadel Kassambara and Fabian Mundt (2020) factoextra: Extract and Visualize the Results of Multivariate Data Analyses. In: R Packag. version 1.0.7
31. Love MI, Huber W, Anders S (2014) Moderated estimation of fold change and dispersion for RNA-seq data with DESeq2. https://doi.org/10.1186/s13059-014-0550-8. Genome Biol
32. Love M, Anders S, Huber W (2017) Analyzing RNA-seq data with DESeq2. Bioconductor
33. Graffelman J, Van Eeuwijk F (2005) Calibration of multivariate scatter plots for exploratory analysis of relations within and between sets of variables in genomic research. Biometrical J. https://doi.org/10.1002/bimj.200510177

34. Gu Z, Eils R, Schlesner M (2016) Complex heatmaps reveal patterns and correlations in multidimensional genomic data. Bioinformatics 32:2847–2849. https://doi.org/10.1093/bioinformatics/btw313
35. Gel B, Serra E (2017) KaryoploteR: An R/Bioconductor package to plot customizable genomes displaying arbitrary data. Bioinformatics 33:3088–3090. https://doi.org/10.1093/bioinformatics/btx346
36. Yu G, Wang LG, Han Y, He QY (2012) ClusterProfiler: An R package for comparing biological themes among gene clusters. Omi A J Integr Biol 16:284–287. https://doi.org/10.1089/omi.2011.0118
37. Walter W, Sánchez-Cabo F, Ricote M (2015) GOplot: An R package for visually combining expression data with functional analysis. Bioinformatics 31:2912–2914. https://doi.org/10.1093/bioinformatics/btv300
38. Chou CH, Shrestha S, Yang CD et al (2018) MiRTarBase update 2018: A resource for experimentally validated microRNA-target interactions. Nucleic Acids Res 46:D296–D302. https://doi.org/10.1093/nar/gkx1067
39. Agarwal V, Bell GW, Nam JW, Bartel DP (2015) Predicting effective microRNA target sites in mammalian mRNAs. https://doi.org/10.7554/eLife.05005. Elife 4:
40. DS AJ M, E L (2012) miRcode: a map of putative microRNA target sites in the long non-coding transcriptome. Bioinformatics 28:2062–2063. https://doi.org/10.1093/BIOINFORMATICS/BTS344
41. Maere S, Heymans K, Kuiper M (2005) BiNGO: A Cytoscape plugin to assess overrepresentation of Gene Ontology categories in Biological Networks. https://doi.org/10.1093/bioinformatics/bti551. Bioinformatics
42. Csardi G, Nepusz T (2006) The igraph software package for complex network research, InterJournal, Complex Systems. InterJournal
43. Meyers RL, Maibach R, Hiyama E et al (2017) Risk-stratified staging in paediatric hepatoblastoma: a unified analysis from the Children's Hepatic tumors International Collaboration. Lancet Oncol 18:122–131. https://doi.org/10.1016/S1470-2045(16)30598-8
44. Czauderna P, Haeberle B, Hiyama E et al (2016) The Children's Hepatic tumors International Collaboration (CHIC): Novel global rare tumor database yields new prognostic factors in hepatoblastoma and becomes a research model. Eur J Cancer 52:92–101. https://doi.org/10.1016/j.ejca.2015.09.023
45. Rivas M, Aguiar T, Fernandes G et al (2021) DNA methylation as a key epigenetic player for hepatoblastoma characterization. Clin Res Hepatol Gastroenterol 45:101684. https://doi.org/10.1016/J.CLINRE.2021.101684
46. Czauderna P, Garnier H (2018) Hepatoblastoma: current understanding, recent advances, and controversies. https://doi.org/10.12688/f1000research.12239.1. F1000Research 7:53
47. Julio C, Wiederkehr IM, Coelho, Sylvio G, Avilla BAW (2012) and HAW Liver tumors in infancy. In: Hepatic Surgery. pp 423–459

48. López-Terrada D, Alaggio R, De Dávila MT et al (2014) Towards an international pediatric liver tumor consensus classification: Proceedings of the Los Angeles COG liver tumors symposium. In: Modern Pathology
49. Lieven O, Knobloch J, Rüther U (2010) The regulation of Dkk1 expression during embryonic development. Dev Biol 340:256–268. https://doi.org/10.1016/j.ydbio.2010.01.037
50. Wang RN, Green J, Wang Z et al (2014) Bone Morphogenetic Protein (BMP) signaling in development and human diseases. Genes Dis 1:87–105
51. Camilleri S, McDonald F (2006) Runx2 and dental development. Eur J Oral Sci 114:361–373
52. Valdivia LE, Young RM, Hawkins TA et al (2011) Lef1-dependent Wnt/β-catenin signalling drives the proliferative engine that maintains tissue homeostasis during lateral line development. Development 138:3931–3941. https://doi.org/10.1242/dev.062695
53. Nunes FD, de Almeida FC, Tucci R, de Sousa SC (2003) Homeobox genes: a molecular link between development and cancer. Pesqui Odontol Bras 17:94–98
54. Pakakasama S, Chen TTL, Frawley W et al (2004) CCND1 polymorphism and age of onset of hepatoblastoma. Oncogene 23:4789–4792. https://doi.org/10.1038/sj.onc.1207499
55. Davies SM (1993) Maintenance of Genomic Imprinting at the IGF2 Locus in Hepatoblastoma.Cancer Res
56. Wirths O, Waha A, Weggen S et al (2003) Overexpression of human Dickkopf-1, an antagonist of wingless/WNT signaling, in human hepatoblastomas and Wilms' tumors. https://doi.org/10.1097/01.LAB.0000059926.66359.BD. Lab Investig
57. Těšínský M, Šimčíková D, Heneberg P (2019) First evidence of changes in enzyme kinetics and stability of glucokinase affected by somatic cancer-associated variations. Biochim Biophys Acta - Proteins Proteomics 1867:213–218. https://doi.org/10.1016/j.bbapap.2018.12.008
58. Hagelkruys A, Sawicka A, Rennmayr M, Seiser C (2011) The biology of HDAC in cancer: The nuclear and epigenetic components. Handb Exp Pharmacol. https://doi.org/10.1007/978-3-642-21631-2_2
59. Crippa S, Ancey P, Vazquez J et al (2017) Mutant CTNNB 1 and histological heterogeneity define metabolic subtypes of hepatoblastoma. EMBO Mol Med. https://doi.org/10.15252/emmm.201707814
60. Wang J, Tian R, Shan Y et al (2020) Metabolomics study of the metabolic changes in hepatoblastoma cells in response to NTCP/SLC10A1 overexpression. Int J Biochem Cell Biol 125:105773. https://doi.org/10.1016/j.biocel.2020.105773
61. Cui X, Wang Z, Li J et al (2020) Cross talk between RNA N6-methyladenosine methyltransferase-like 3 and miR-186 regulates hepatoblastoma progression through Wnt/β-catenin signalling pathway. Cell Prolif 53. https://doi.org/10.1111/cpr.12768
62. Vastrad B, Vastrad C, Kottursheti I (2020) Identification of potential core genes in hepatoblastoma via bioinformatics analysis. medRxiv

63. Honda S, Chatterjee A, Leichter AL et al (2020) A MicroRNA Cluster in the DLK1-DIO3 Imprinted Region on Chromosome 14q32.2 Is Dysregulated in Metastatic Hepatoblastomas. Front Oncol. https://doi.org/10.3389/fonc.2020.513601
64. Beck A, Eberherr C, Hagemann M et al (2016) Connectivity map identifies HDAC inhibition as a treatment option of high-risk hepatoblastoma. Cancer Biol Ther. https://doi.org/10.1080/15384047.2016.1235664
65. Ge X, Chen Y, Liao X et al (2013) Overexpression of long noncoding RNA PCAT-1 is a novel biomarker of poor prognosis in patients with colorectal cancer. Med Oncol. https://doi.org/10.1007/s12032-013-0588-6
66. Pan YF, Qin T, Feng L, Yu ZJ (2013) Expression profile of altered long non-coding RNAs in patients with HBV-associated hepatocellular carcinoma. J Huazhong Univ Sci Technol - Med Sci. https://doi.org/10.1007/s11596-013-1078-y
67. Sun W, Wu Y, Yu X et al (2013) Decreased expression of long noncoding RNA AC096655.1-002 in gastric cancer and its clinical significance. Tumor Biol. https://doi.org/10.1007/s13277-013-0821-0
68. Qiao HP, Gao WS, Huo JX, Yang ZS (2013) Long non-coding RNA GAS5 Functions as a tumor suppressor in renal cell carcinoma. Asian Pac J Cancer Prev. https://doi.org/10.7314/APJCP.2013.14.2.1077
69. Magrelli A, Azzalin G, Salvatore M, Viganotti M, Tosto F, Colombo T, Devito R, Di Masi A, Antoccia A, Lorenzetti S, Maranghi F, Mantovani A, Tanzarella C, Macino G, Taruscio D (2009) Altered microRNA Expression Patterns in Hepatoblastoma Patients. Transl Oncol 2:157–163. https://doi.org/https://doi.org/10.1593/tlo.09124
70. Gyugos M, Lendvai G, Kenessey I et al (2014) MicroRNA expression might predict prognosis of epithelial hepatoblastoma. Virchows Arch 464:419–427. https://doi.org/10.1007/s00428-014-1549-y
71. Wu JF, Ho MC, Ni YH et al (2020) Dysregulation of liver developmental microRNA contribute to hepatic carcinogenesis. J Formos Med Assoc 119:1041–1051. https://doi.org/10.1016/j.jfma.2019.09.018
72. Chuang KH, Whitney-Miller CL, Chu CY et al (2015) MicroRNA-494 is a master epigenetic regulator of multiple invasion-suppressor microRNAs by targeting ten eleven translocation 1 in invasive human hepatocellular carcinoma tumors. Hepatology 62:466–480. https://doi.org/10.1002/hep.27816
73. Liu K, Liu S, Zhang W et al (2015) miR-494 promotes cell proliferation, migration and invasion, and increased sorafenib resistance in hepatocellular carcinoma by targeting PTEN. Oncol Rep 34:1003–1010. https://doi.org/10.3892/or.2015.4030

Tables

Table 1 to 3 are available in the Supplemental Files section.

Figures

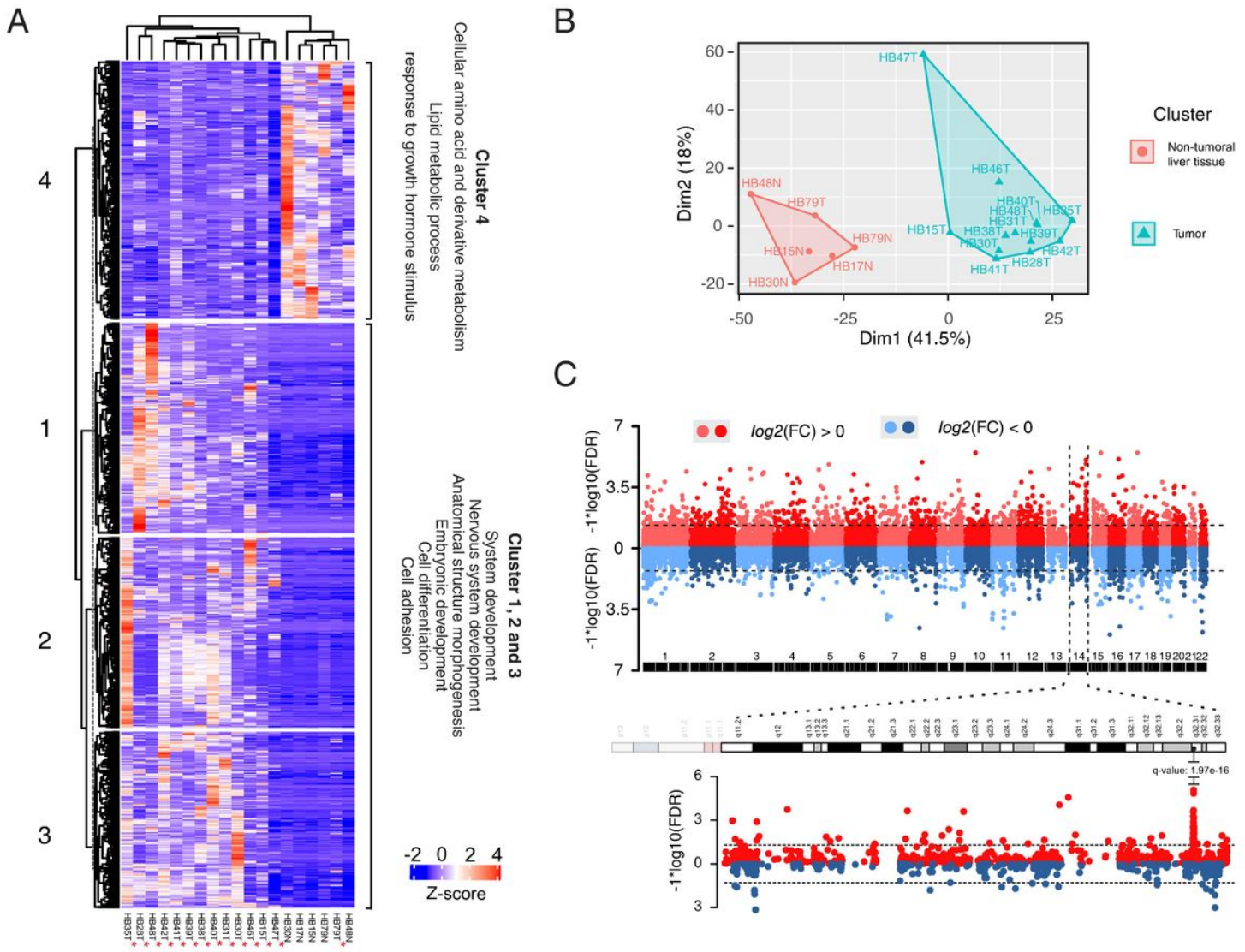

Figure 1

RNASeq gene expression analysis of hepatoblastomas.

(A) A heatmap representation of gene expression of HBLs (T; samples with a red asterisk) and control liver samples (N); gene expression was normalized by Z score, and a legend of colors in the figure indicates downregulated genes (blue) and upregulated genes (red). Four major clusters were separated using the k-means method; the main biological processes enriched in Clusters 1, 2, 3 and 4 are indicated at right.

(B) PCA of differentially expressed genes highlighted the two identified clusters and the respective grouped samples; the cluster 1 samples are represented by solid red dots (control livers: HB15N, HB17N, HB30N, HB48N, and HB79N) and the cluster 2 samples (HBLs: HB15T, HB28T, HB30T, HB31T, HB35T, HB38T, HB39T, HB40T, HB41T, HB42T, HB46T, HB47T, HB48T, and HB79T) are represented by blue triangles.

(C) Representation of the genomic mapping of the differentially expressed genes along the chromosomes, from 1 to 22. Dots in red and blue represent genes with $\log_2$ fold-change above (upregulated) or below (downregulated) 0, respectively. One peak of upregulated genes can be visualized at the 14q32 cytoband (detailed below the plot).

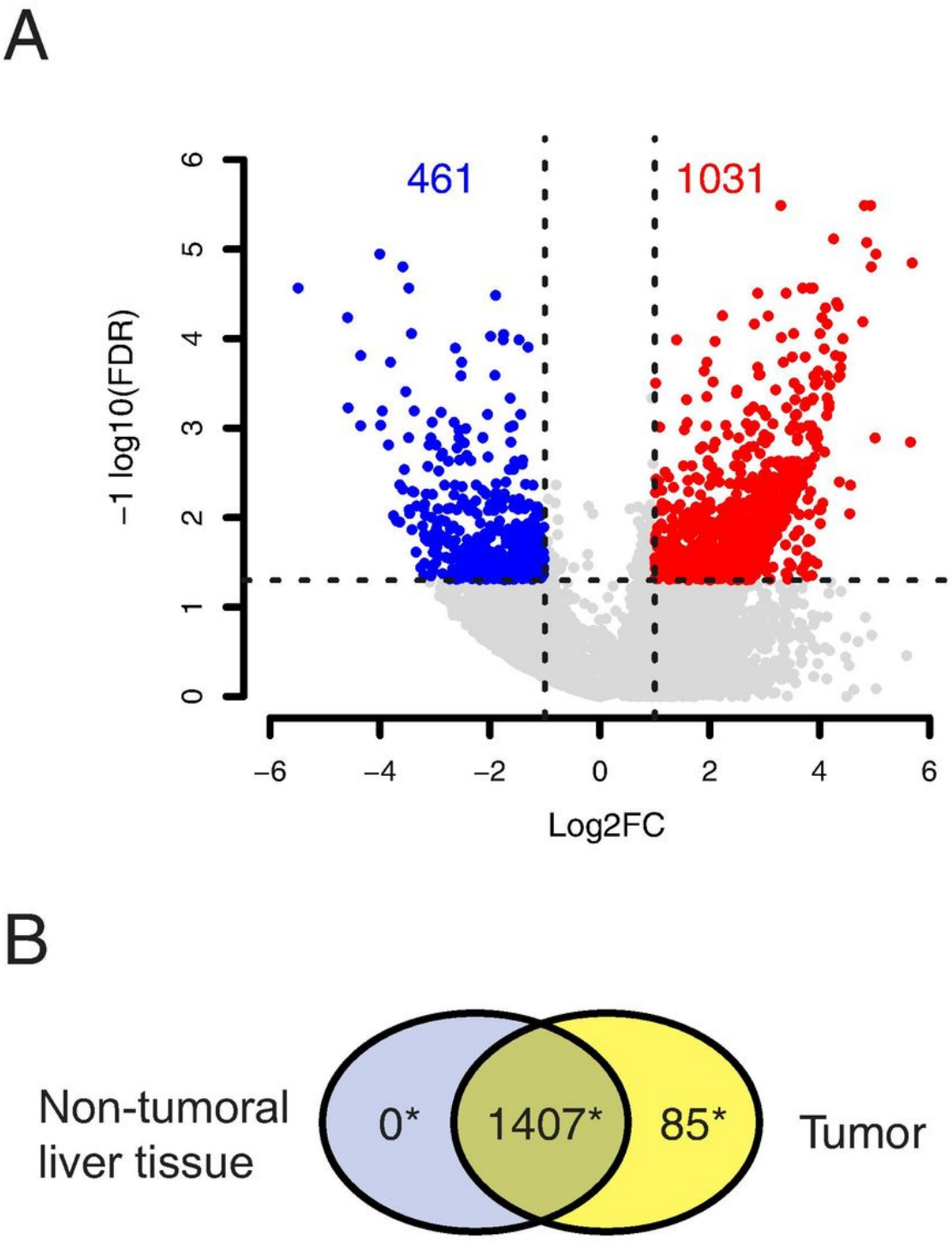

Figure 2

Differentially expressed genes in HBL transcriptome.

(A) A volcano plot showing all expressed genes in HBL samples. Genes differentially expressed (DEG) in HBLs compared to control livers with statistical significance and $\log_2$FC < -1 or > 1 are represented as blue (down-regulated genes) or red (up-regulated genes) dots; the gray-colored dots depict genes with no statistical differences. (B) A Venn diagram showing the groups of shared and exclusive expressed transcripts of HBLs and controls.

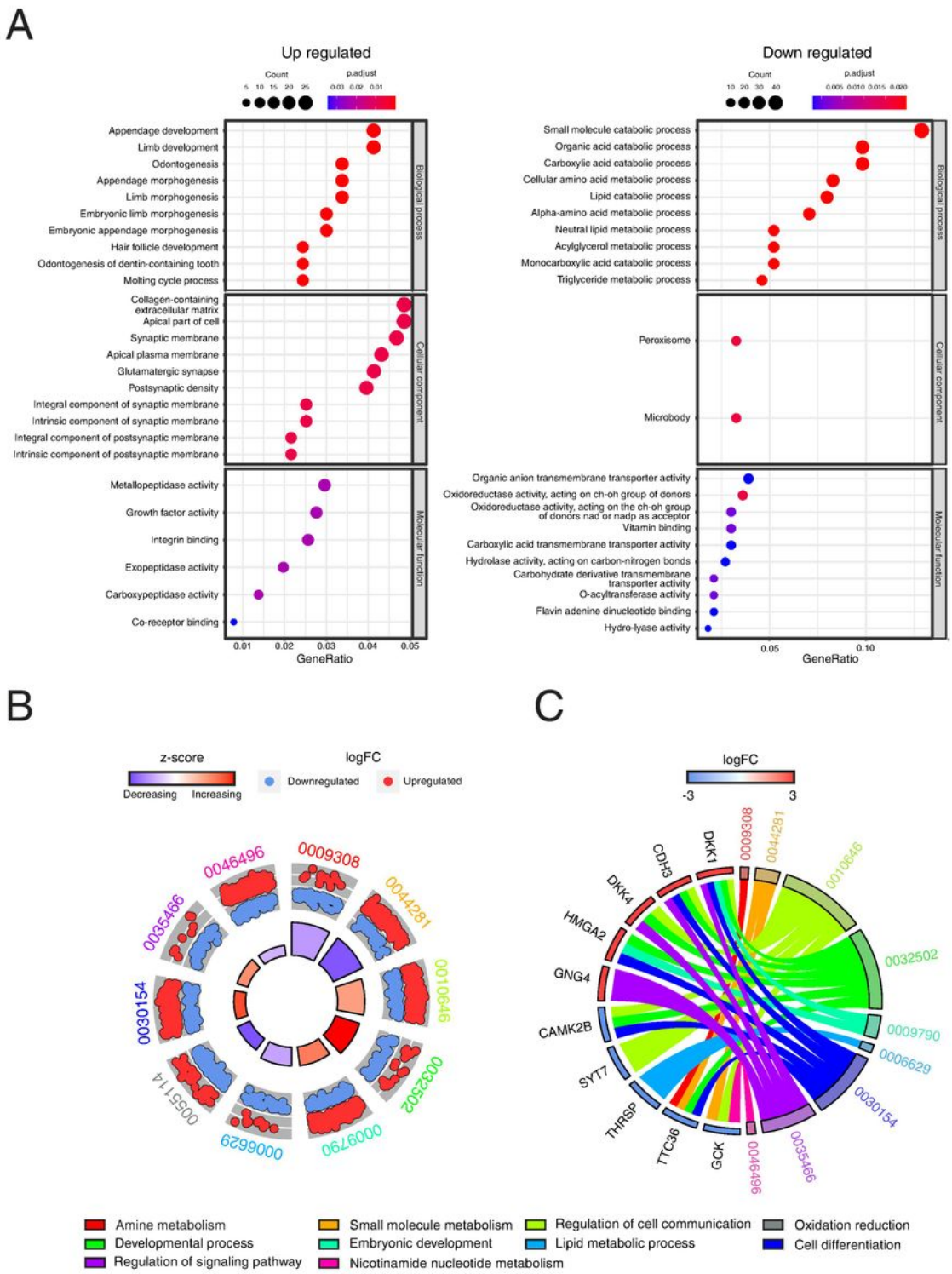

Figure 3

Enrichment analysis of the differentially expressed genes of the transcriptome of hepatoblastomas.

(A) Dotplot presenting the top ten functional enrichment analyses of DEGs in biological process, cellular component, and molecular function in HBL samples. The dot size refers to the number of genes in the

DEG list associated with the event, and the color is associated with the p-adj value. At left, upregulated genes, at right, downregulated genes.

(B) A GOCircle showing the biological processes enriched for the differentially expressed genes of HBLs. The outer circle shows a scatter plot of the log_2FC for each gene under the gene ontology (GO) terms; red dots indicate upregulated genes and blue dots, downregulated genes. The inner-circle shows the z-score, a measure of up-or downregulation predominance of each identified process. GO identification – 0009308: Amine Metabolic process; 0044281: Small molecule metabolic process; 0010646: Regulation of cell communication; 0032502: Developmental process; 0009790: Embryonic development; 0006629: Lipid metabolic process; 0055114: Oxidation-reduction; 0030154: cell differentiation; 0035466: Regulation of signaling pathway; 0046496: Nicotinamide nucleotide metabolic process.

C) The chord diagram shows ten out of 50 genes with major expression changes associated with nine of the ten biological processes of (B). Blue and red bars next to the genes represent the down or upregulated fold-change, respectively. Biological processes are identified by specific colors; the association with each gene is demonstrated by the connecting chord.

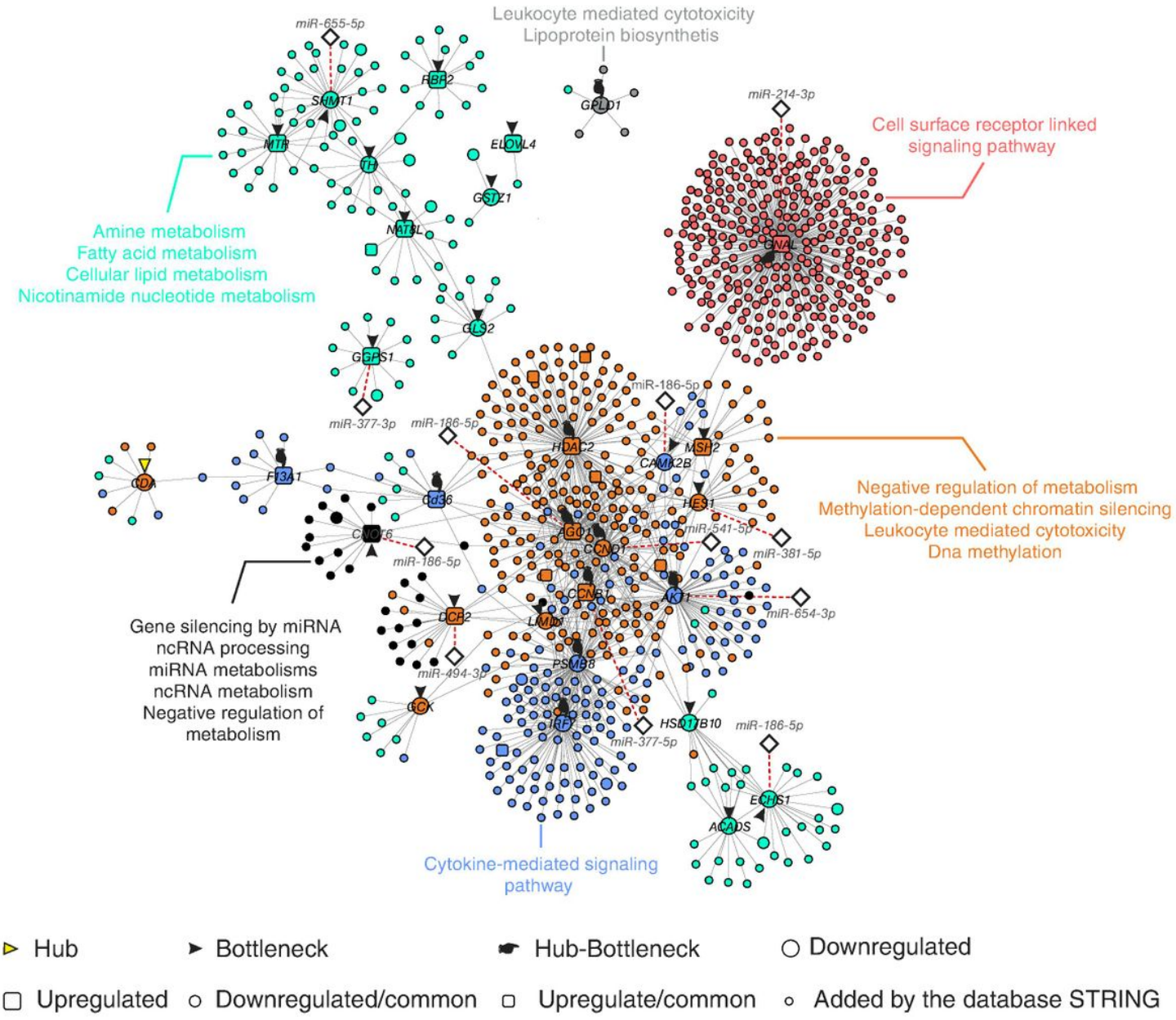

Figure 4

Protein-protein interaction network of the differentially expressed protein-coding genes. PPI highlighting centralities and proteins that interact directly with these nodes. Colors represent different biological processes. Square and round dots indicate nodes up-and down-regulated, respectively. Centrality measures showed that the networks were composed of one hub protein (y triangle), nineteen bottleneck nodes (black triangle), and eleven hub-bottleneck (black finger). miRNAs are represented by blank diamonds.

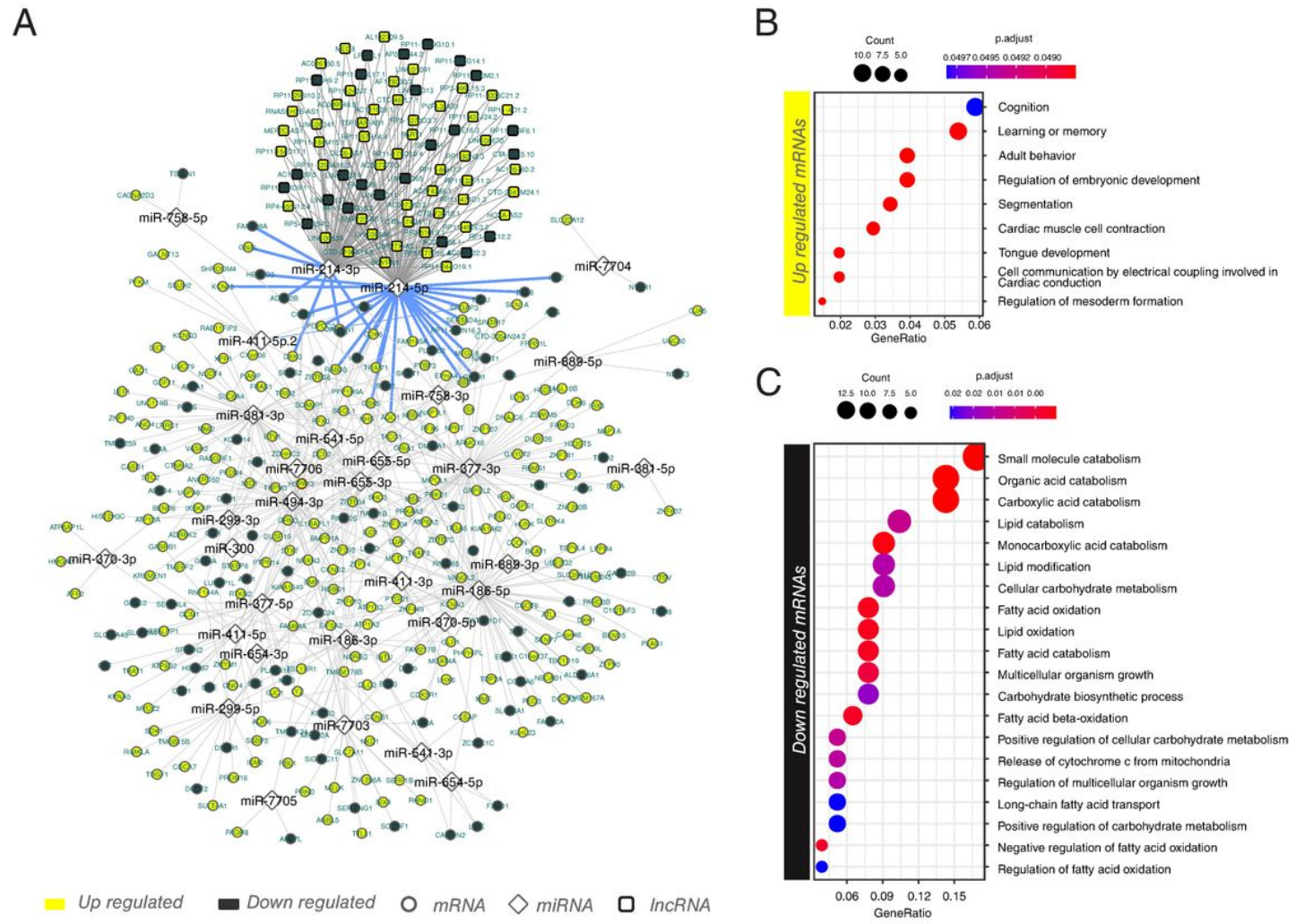

Figure 5

Association between miRNA and protein-coding genes in HBLs.

(A) miRNA-mRNA interaction network. Yellow dots represent upregulated mRNAs in HBL, black dots represent downregulated mRNAs. miRNA: micro-RNA; mRNA: messenger RNA.

(B) and (C) Dotplot of biological processes. The dot size represents the number of mRNAs in the network associated with the process; the dot color is linked to the level of the adjp-value. The gene ratio refers to the value of the number of mRNAs associated with the biological process by the total number of mRNAs in the network. In (B) are the upregulated mRNAs and in (C) are the downregulated mRNAs.

Supplementary Files

This is a list of supplementary files associated with this preprint. Click to download.

- SUPPLEMENTARYMATERIAL.docx
- Supplementarytables.xlsx
- Table1.pdf
- Table2.pdf
- Table3.pdf